Experimental Characterization of Traditional Composites Manufactured by Vacuum-Assisted Resin-Transfer Molding

Volkan Cecen,[1] Mehmet Sarikanat[2]

[1]*Department of Mechanical Engineering, Dokuz Eylul University, 35100 Bornova, Izmir, Turkey*
[2]*Department of Mechanical Engineering, Ege University, 35100 Bornova, Izmir, Turkey*

Received 21 December 2006; accepted 28 July 2007
DOI 10.1002/app.27235
Published online 25 October 2007 in Wiley InterScience (www.interscience.wiley.com).

ABSTRACT: The primary purpose of this study is to investigate the anisotropic behavior of different glass-fabric-reinforced polyester composites. Two commonly used types of traditional glass fabrics, woven roving fabric and chopped strand mat, have been used. Composite laminates have been manufactured by the vacuum infusion of polyester resin into the fabrics. The effects of geometric variables on the composite structural integrity and strength are illustrated. Hence, tensile and three-point-bending flexural tests have been conducted at different off-axial angles (0, 45, and 90°) with respect to the longitudinal direction. In this study, an important practical problem with fibrous composites, the interlaminar shear strength as measured in short-beam shear tests, is discussed. The most significant result deduced from this investigation is the strong correlation between the changes in the interlaminar shear strength values and fiber orientation angle in the case of woven fabric laminates. Extensive photographs of fractured tensile specimens resulting from a variety of uniaxial loading conditions are presented. Another aim of this work is to investigate the interaction between the glass fiber and polyester matrix. The experiments, in conjunction with scanning electron photomicrographs of fractured surfaces of composites, are interpreted in an attempt to explain the interaction between the glass fiber and polyester. J Appl Polym Sci 107: 1822–1830, 2008

Key words: composites; electron microscopy; mechanical properties

INTRODUCTION

In many applications in the reinforced plastics industry, glass fabrics and woven rovings provide mechanical properties in the laminate that are much greater than those required, apart from stiffness, and for such applications, a cheaper material is adequate.[1] Glass fabrics in the form of unidirectional rovings, woven rovings, and chopped strand mats are the most widely used sheetlike materials for the reinforcement of polymers. Composites made with these fabrics may be classified as traditional composites because of their use over many years, and they have remained popular because glass fiber is inexpensive and usually provides good in-plane mechanical properties.[2]

The effects of different variables (manufacturing techniques, geometries, and types of fibers) on the mechanical properties of woven fabric laminates have been recently investigated experimentally.[3–7] Yang et al.[8] investigated experimentally the mechanical properties and failure mechanisms of through-the-thickness stitched plain-weave glass fabric–epoxy composites. The reliable prediction of properties of composite materials has received considerable attention in recent years. Many of these studies, both theoretical and experimental, have examined the individual properties of woven-fabric-reinforced polymer composites, and some of the predictive models available for determining them have been extensively reviewed elsewhere.[9]

Although there exists in the literature a large knowledge base for the mechanical properties of glass-mat-reinforced thermoplastics,[10–18] only limited information is available on the properties of composites having glass mat/thermoset matrix combinations.[19,20]

In this study, polyester resin was infused to impregnate a glass fiber preform through vacuum-assisted resin-transfer molding (VARTM). VARTM and the patented Seemann composite resin-infusion molding process[21,22] have been developed as alternative, low-cost methods for the manufacture of composite structures. The resin-infusion processes lend themselves to the use of nearly net-shaped textile preforms manufactured through a variety of automated textile processes such as knitting and braiding.[23] The challenge facing the resin-infusion techniques is to design a robust process that will consistently ensure the complete infiltration and cure of a geometrically complex shape preform with the high fiber volume fraction needed for structural

Correspondence to: V. Cecen (volkan.cecen@deu.edu.tr).

TABLE I
Compositions of the Traditional Fiberglass Composites

Composite	Areal density of fabric (g/m^2)	Number of fabric layers	Laminate thickness (mm)
Woven roving fabric	300 g/m^2	12	3.05
Glass mat fabric	450 g/m^2	12	5.98

applications. One major disadvantage of resin-infusion processes is that they require long-duration and high-temperature cure cycles to cure the resin-saturated preforms fully.

The major goal of the research described in this article was to study the anisotropy of polyester composites reinforced with traditional glass fabric. The study of anisotropy was carried out to investigate the effects of geometric variables, such as the directions of fiber orientation, on the structural integrity and strength of laminates made with woven roving fabric and chopped strand mat. Hence, tensile, three-point-bending, and short-beam shear tests were conducted up to failure on specimens. The fabric composites were tested in three directions: at 0, 45, and 90°. In addition to the extensive efforts in elucidating the variation in the mechanical properties of polyester laminates built from woven roving fabric and chopped strand mat blankets, the work presented here focuses also on the types of interactions that are established between the polyester and glass fiber. Scanning electron microscopy (SEM) was also helpful and was additionally used to describe the morphological features of fractured surfaces of glass–polyester composites.

EXPERIMENTAL

Materials and sample preparation

Two commonly used varieties of fiberglass composite were made that contained woven roving and chopped strand mat. The compositions of these materials are given in Table I. Figure 1(a,b) shows scanned images of pieces of woven roving glass fabric and glass mat fabric. The fabric parameters, as specified by the manufacturer, are also shown in Table I.

The Polipol (Poliya Polyester ve Yardimcı Maddeler Sanayi AŞ, Istanbul, Turkey) polyester 383-T resin system was used as the resin in the composite. The resin (specific gravity = 1.11, Brookfield viscosity = 950), which was an isophthalic acid type resin, was mixed before VARTM with the catalyst cobalt octoate (0.35 pph in a 41% solution of white spirit), the retarder 2,4-pentanedione (0.10 pph), and methyl ethyl ketone peroxide (2.2 pph in a 40% dimethyl phthalate solution).

The VARTM equipment at GOVSA Composites, Ltd., (Izmir, Turkey), was used to manufacture composite plates. Two types of composite plates with different fiber volume fractions, shown in Table II (the data, obtained by a resin burn-off method, are the reported mean values from the manufacturer), were used for the test specimens. In the VARTM process, the entire fiber-reinforced polymer composite was produced in a operation in which resin was injected with the assistance of vacuum (Fig. 2). The fibrous preform was laid on top of the tool and was covered by a distribution medium with a high in-plane permeability to accelerate the in-plane flow. The resin inlet was placed in the middle of the stack and was connected to a resin tank as a resin injection gate. A vacuum pump was connected to a vacuum port, which was placed on a glass plate, with a polyethylene tube (Fig. 2). With the vacuum bag tightly sealed and the injection gate closed, the vacuum pump was turned on. Vacuum was drawn through the vacuum line to remove air from the mold cavity and induce fiber compaction under atmospheric pressure. Then, the injection gate was opened to allow resin infusion into the highly permeable distribution medium under atmospheric pressure. When the preform was completely infiltrated, the injection tube was clamped, and the infused panel was left to cure for 24 h at room temperature and *in vacuo*.

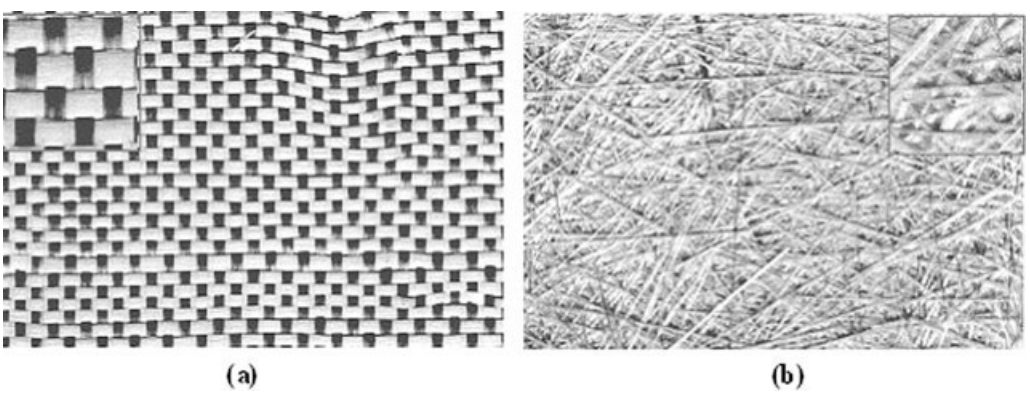

Figure 1 Fabric samples: (a) woven roving fabric and (b) glass mat fabric.

TABLE II
Mechanical Properties of Glass Fiber/Polyester Composites in Different Directions

Composite	Fiber volume fraction (%)	Test direction	Tensile modulus (GPa)	Tensile strength (MPa)	Elongation at break (%)	Flexural modulus (GPa)	Flexural strength (MPa)	ILSS (MPa)
Woven roving fabric	49.2 ± 1.8	Machine	16.470 ± 0.7	313.05 ± 13	2.5310 ± 0.1	15.404 ± 0.7	310.85 ± 13	14.559 ± 0.6
		Bias	7.8540 ± 0.4	106.55 ± 5.8	8.9910 ± 0.5	6.5510 ± 0.4	100.06 ± 5.6	5.4211 ± 0.3
		Cross	14.459 ± 0.7	203.76 ± 12	1.3580 ± 0.1	15.892 ± 0.7	294.81 ± 13	13.908 ± 0.6
Glass mat fabric	37.6 ± 1.6	Machine	12.028 ± 0.6	167.99 ± 6.5	1.6110 ± 0.1	10.028 ± 0.5	276.80 ± 13	22.036 ± 0.8
		Bias	10.742 ± 0.5	161.40 ± 6.3	1.6700 ± 0.1	10.616 ± 0.6	242.07 ± 12	21.685 ± 0.8
		Cross	10.989 ± 0.6	174.68 ± 6.9	1.7470 ± 0.1	11.087 ± 0.5	309.53 ± 13	25.790 ± 0.9

The quoted data are all average results taken from a minimum of six tests. The values after ± refer to the standard uncertainty of the measurement.

The testing specimens were cut as illustrated in Figure 3. The final dimensions of each test specimen are identified as in Figure 4.

Figure 3 illustrates the test directions performed on the specimens; the machine direction (MD) is the flow direction of fabric in the machine during production, whereas the bias direction (BD) and cross direction (CD) are 45 and 90° with respect to MD, respectively. It is well known that in an orthogonal woven fabric, MD and CD are called the warp and weft directions, respectively.

Tensile strength testing

The tensile experiments were conducted with reference to ASTM D 3039 on a Shimadzu Autograph AG-G series universal testing machine with a video extensometer system (Shimadzu DVE-101/201 noncontact video extensometer) and with Trapezium (advanced software for materials testing) for machine control and data acquisition. ASTM D 3039 was applied to prepared specimens to obtain experimental elastic moduli and tensile strengths in MD, CD, and BD. Four rectangular tabs to be used with the tensile specimens were produced from carbon-fiber-reinforced epoxy with the lay-up $[0/90]_s$ (symmetric cross ply laminate) and were bonded to the gripping length of each test specimen with a cold-hardening epoxy resin. Tensile tests were performed at a constant crosshead speed of 2 mm/min at room temperature in air. Six tests were made for each material per orientation.

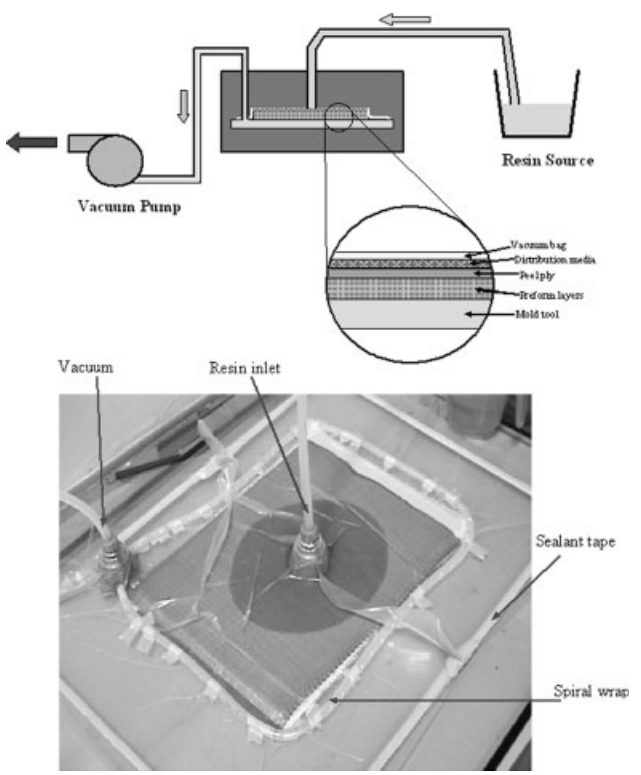

Figure 2 VARTM process and fabrication setup.

Flexural test

One of the commonest experiments used to characterize materials under flexural conditions is the three-point-bending test. Specimens were machined from flat panels with a high-speed diamond saw with a 50/50 mix of water and ethylene glycol coolant. This machining operation resulted in constant-width specimens having very smooth cuts. The gauge lengths for the three-point-bending test were

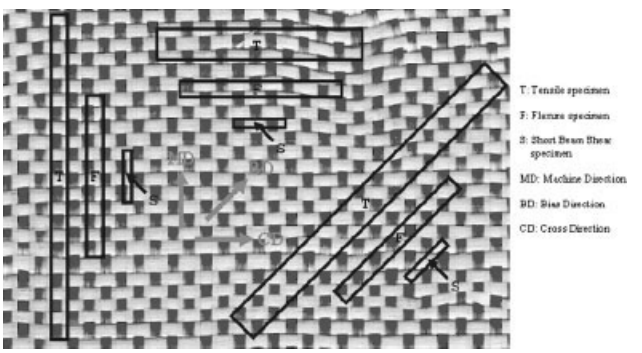

Figure 3 Location of test pieces cut from the laminates used for mechanical testing and directions of measurements.

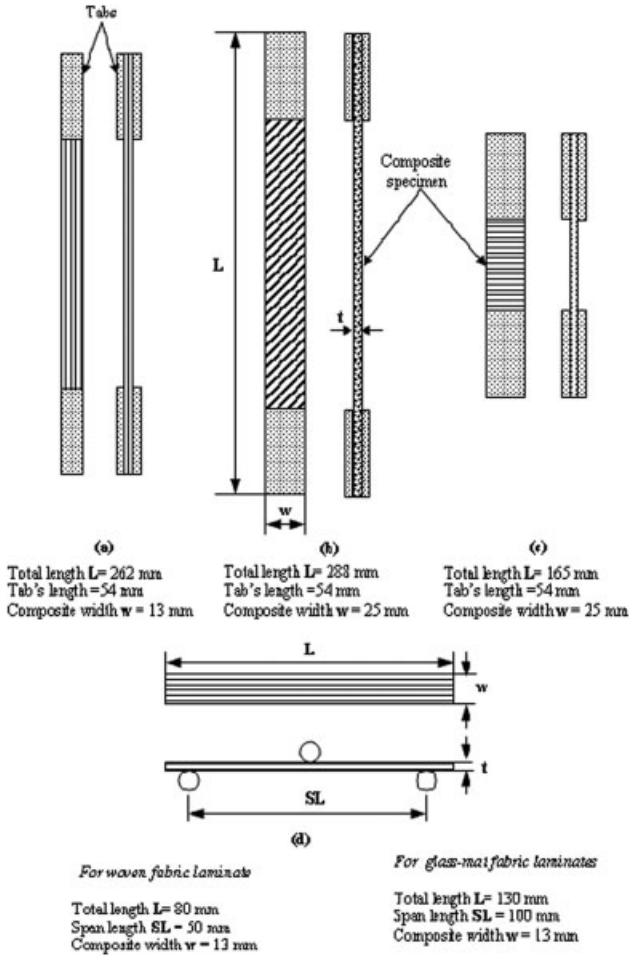

Figure 4 Schematic diagrams of the testing geometries: (a) longitudinal, (b) off-axis, (c) transverse tension, and (d) flexural.

determined according to ASTM Standard D 790 and were set to 100 mm for all the composite specimens. The flexural strength (σ_f) can be derived from the simple beam theory as follows:

$$\sigma_f = \frac{3PL}{2wt^2} \tag{1}$$

where P is the applied load that leads the specimen to rupture, L is the support span, w is the specimen width, and t is the specimen thickness.

For the case in which the three-point flexural specimen is not strain-gauged, the flexural modulus (E_f) can be determined from the slope of the initial straight-line part of the load–deflection curve by means of this equation:

$$E_f = \frac{L^3}{4wt^3}\frac{\Delta P}{\Delta \delta} \tag{2}$$

where $\Delta P/\Delta\delta$ represents the slope of the force–displacement curve.

Short-beam shear test

To determine the interlaminar shear strength of the composites, short-beam shear tests were performed according to ASTM 2344 (''Apparent Interlaminar Shear Strength of Parallel Fiber Composites by Short-Beam Method''). A sliding-roller three-point-bending fixture, which included a loading pin (diameter = 6.4 mm) and two support pins (diameter = 3.2 mm), was used for the room-temperature short-beam shear tests. The test fixture was mounted in a 5-kN-capacity, screw-driven load frame. The apparent interlaminar shear strength of the composites was determined from samples that were tested with a support span/sample thickness ratio of 5 : 1. The simply supported specimens allow lateral motion, and a line load was applied at the mid-span of the specimens. The apparent shear strength (V) was then calculated as follows:

$$V = 0.75\left(\frac{P_{\max}}{wt}\right) \tag{3}$$

where $P_{\max}$ is the failure load. Further details of the test procedures are given in ASTM 2344.

SEM observation

The fracture surfaces of tensile-tested specimens were examined with a JEOL (Jeol Ltd., Tokyo, Japan) JSM 6060 scanning electron microscope at an excitation voltage equal to 20 keV in the secondary electron mode. To reduce the extent of sample arcing, the samples were coated with a thin layer of metallic gold in a Polaran SC7620 automatic sputter coater (VG MicroTech, UK) before examination by SEM.

RESULTS AND DISCUSSION

Experimental results and discussions of the mechanical properties

Tensile properties

Comparisons of the values of the tensile strength determined experimentally with the tensile specimens cut at different angles from the same woven roving glass/polyester laminate are shown in Table II.

The anisotropy may be a result of the orthogonal arrangement of the fibers in the woven plain-weave fabrics that are made by the interlacing of two yarn systems at a 90° angle. From the stress–strain curves shown in Figure 5(a), it can be seen that the strength of the woven fabric composite is greater in the two orthogonal directions (in this particular instance, MD and CD) in which each warp and weft yarns lie than in any other direction. It can be

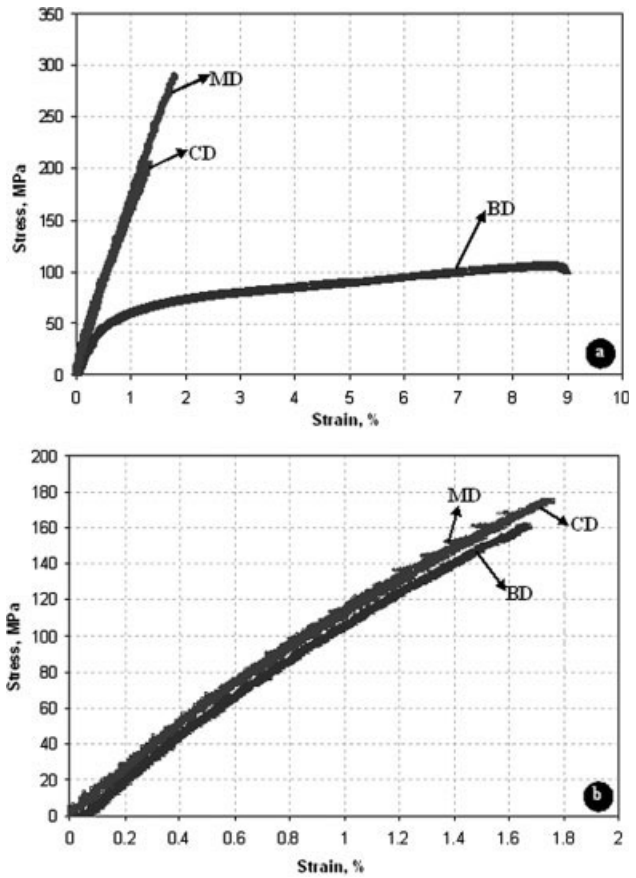

Figure 5 Tensile stress–strain curves of laminates in different directions: (a) woven roving fabric and (b) glass mat fabric laminate.

observed from Table II that for specimens made from woven roving glass fabric laminates, the experimental data do not allow for an adequate description of the orthogonal model. A somewhat surprising feature is that the strength in MD is about 54% higher than that in CD, whereas the stiffness differs merely by a few percent. A potential explanation for the difference between the tensile strength values in MD and CD could be that the laying up of the fabric in composite production is not truly aligned in the desirable direction because the nominal warp and weft directions of the fibers are not controlled during the laminate fabrication by the VARTM process. Another point that should be made here is that deviation from the perfect alignment of fibers accumulates from the precision in cutting the laminates for specimens with desired directions.

The experimental results show that the delamination does not occur at the mid-plane in the case of BD and CD but instead occurs in the outer first layer, as shown in Figure 6(a), whereas extensive delamination occurred in a specimen subjected to tension in MD.

The large increase in the elongation at break of woven fabric composites tested in BD suggests that the effect of the knee in the stress–strain curve on the break strain may be much more significant in the matrix-controlled failure mode (in the case of BD) than in the fiber-controlled failure modes (in the case of MD and CD; Table II). Figure 5(a) clearly indicates that once the knee point is passed, the composite may be capable of significant further extension, although it is permanently damaged.

As would be expected, glass mat fabric laminates in which the fibers are randomly distributed are isotropic. The experimental results show that the tensile strength values were, therefore, the same in all test directions performed on the composites [Fig. 5(b)]. Resistance to delamination can also be increased by the use of a perfectly random arrangement of fibers, such as a chopped strand mat. No delamination was observed in the glass mat fabric/polyester laminate under tension along MD, BD, and CD [Fig. 6(b)].

Flexural properties

Catastrophic failure was not observed in the woven roving fabric or in the glass mat fabric laminates. The specimens exhibited a more localized damage region at the top side of the beam by compression and at the bottom side by tension. From a closer observation of the tested specimens, it can be revealed that there was some visible interplane slippage and crack initiation in the mid-plane.

It can be observed from Table II and Figure 7(a) that specimens made from woven roving glass-fabric-reinforced polyester in MD exhibited the highest loading capacity with a ultimate strength of 310.8 MPa, which is 16 MPa higher than the 294.8-MPa loading capacity of the specimens in CD. Similar comments can be made about the discrepancies between the flexural strength/mid-span deflection responses of all specimens in these directions from experiments, just as for the results on the tensile properties of the woven fabric composite laminates in the same directions. Figure 7(a) shows that two of the three experimental curves (MD and CD) reached a peak strength before failing and had similar initial elastic moduli up to cracking. The specimen in BD was the least efficient beam in this group with an ultimate strength of 100 MPa. As illustrated in Figure 7(a), more than 67% of the laminate strength was lost, probably because of the matrix-controlled failure mode.

Perhaps the most significant result of this investigation is the surprisingly strong correlation between the flexural strength and the nonplanar feature of the glass mat fabric laminate. It is interesting to note that the strengths of the isotropic laminate in test

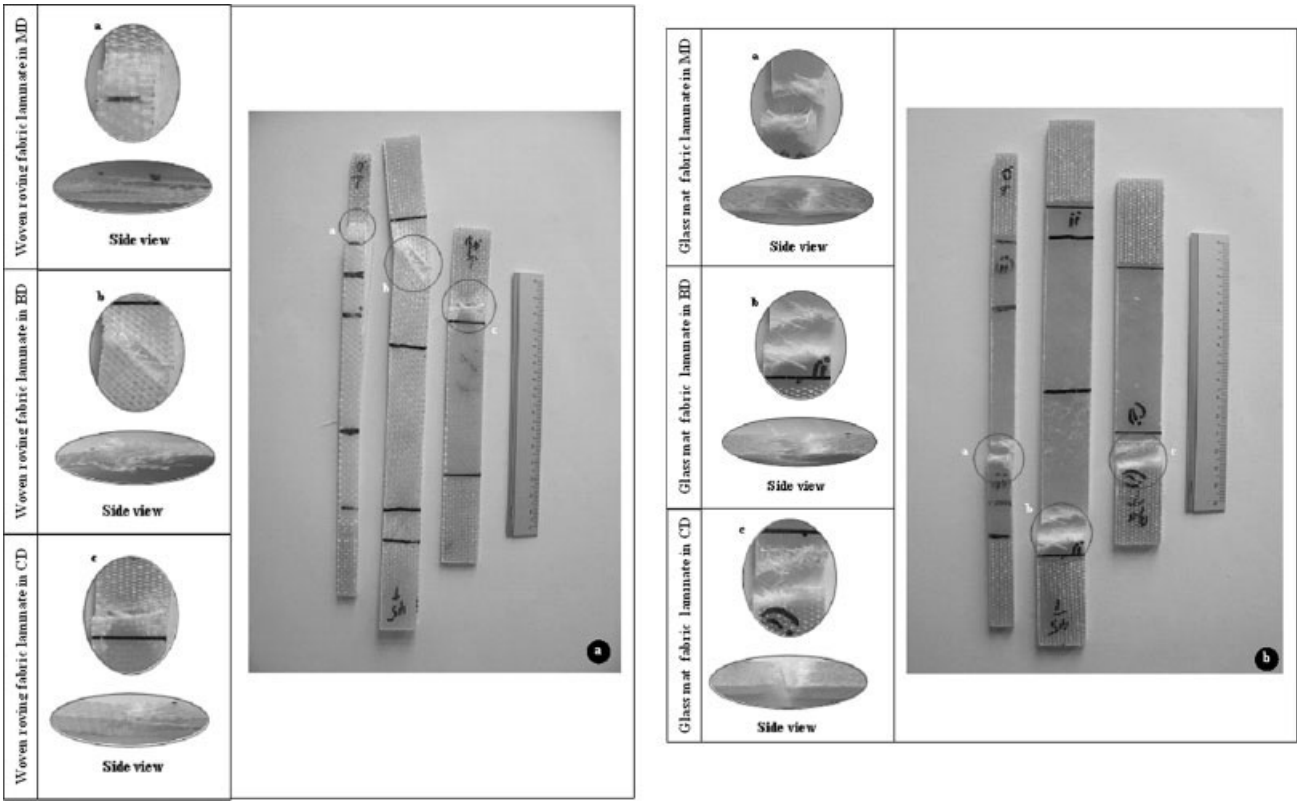

Figure 6 Photographs showing side and front views of representative failures loaded in tension along MD, BD, and CD for laminates produced from (a) woven roving fabric and (b) glass mat fabric laminate.

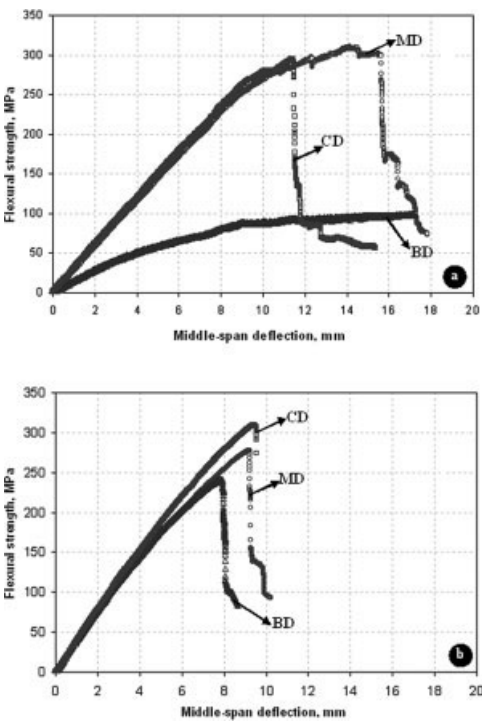

Figure 7 Flexural strength–deflection curves of laminates in different directions: (a) woven roving fabric and (b) glass mat fabric laminate.

directions performed on the composites are not equal [Fig. 7(b)]. It might be thought that when the fiber beds are compressed during vacuum bagging, considerable elastic deformation takes place in the individual fibers or bundles, primarily through bending. It is believed that the local inhomogeneities are made permanent when the polymeric matrix solidifies. These local inhomogeneities may be thought to be responsible for the variation of the flexural strength in all the considered test directions. Ericson and Berglund[24] suggested that the major reason for the insensitivity of the mechanical properties to differences in the microstructure is the inhomogeneity of the materials. They agreed that local inhomogeneities, such as low fiber content, very high fiber content with poor melt impregnation, or unfavorable fiber orientation, rather than the general microstructure of the material, will control the mechanical properties.

Short-beam shear test results

Failure occurs suddenly in a macroscopically brittle mode by crack initiation and propagation. A sharp drop in the load–displacement curves and an audible cracking sound accompany catastrophic delami-

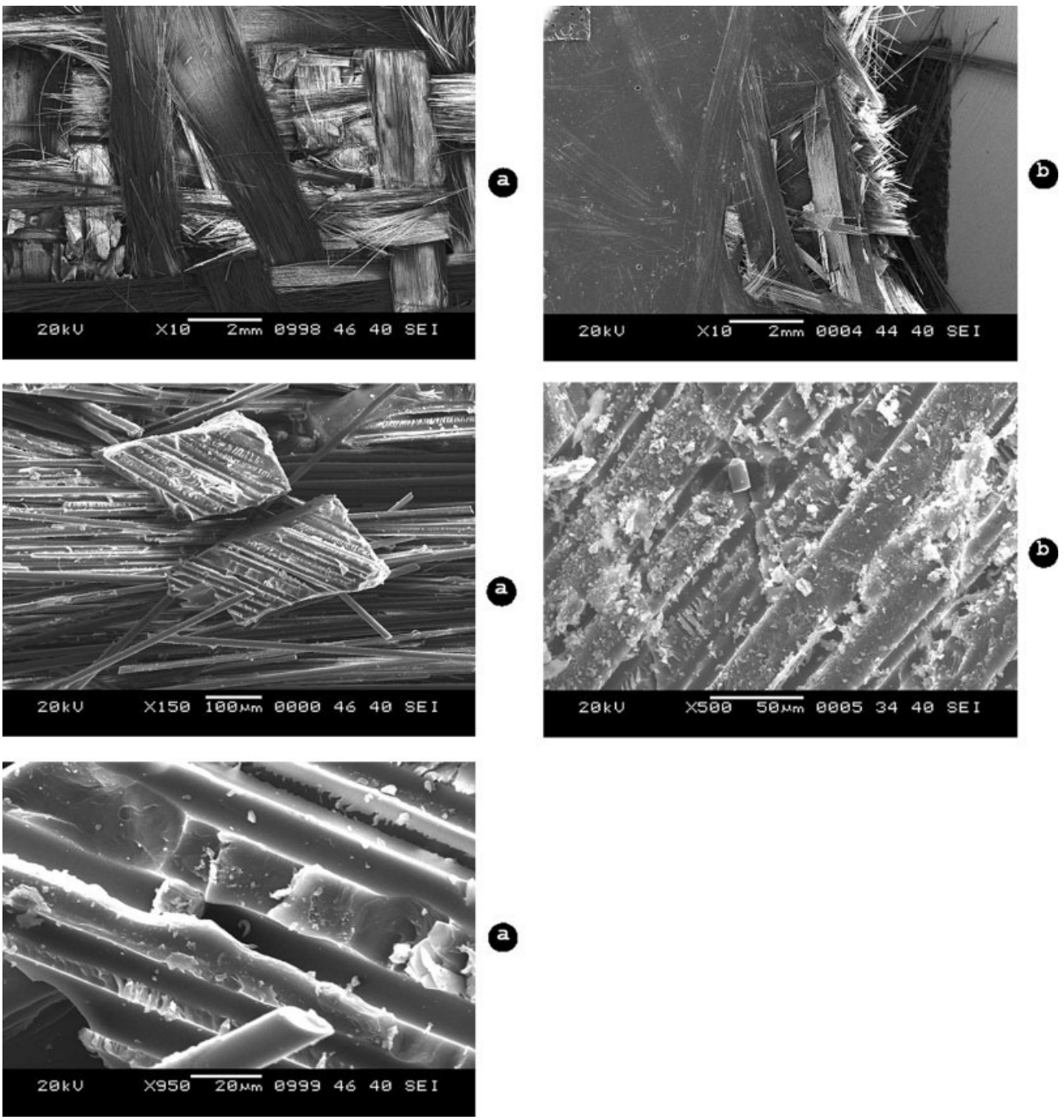

Figure 8 Representative SEM images of the breakage region for (a) woven roving fabric and (b) glass mat fabric laminate that were tensile-tested in MD (at different magnification levels).

nation. In a few tests, failure was not visible at the time of the load drop, but upon the removal of the specimen or with slightly higher displacement, it manifested visibly.

A comparison of the results with data in Table II suggests that polyester composites fabricated from woven roving glass fabric are more susceptible to interlaminar shear strength degradation as a function of test directions than composites produced with the glass mat fabric. Table II shows that specimens made from woven roving glass-fabric-reinforced polyester in BD exhibited the lowest loading capacity with an ultimate strength of 5.4 MPa, which is 169 and 157% lower than the 14.6- and 13.9-MPa loading capacities of the specimens in MD and CD, respectively. The aforementioned results of this investigation demonstrate that, contrary to the general belief that the matrix-dominated property of the

interlaminar shear strength (ILSS) is confirmed by its independence of the fiber orientation, the nominal warp and weft directions of the fibers have a significant effect on the recorded values of the interlaminar shear strengths (Table II).

Observed results from the experiment suggest that the strengths in the three-point flexural test are much higher than those in the short-beam shear test in all the considered directions (Table II).

Fractographic analysis

The fracture surface of composites was observed under different moderate magnification levels after the measurement of the tensile tests in MD (Fig. 8).

Polyester composites made from woven roving glass fabric showed clean holes in the matrix and uncoated fiber surfaces [Fig. 8(a)]. The fiber surfaces were almost completely devoid of matrix material, and this indicated extensive interfacial failure. In addition, there was little matrix material between the fibers on the postfracture surface; that is, the fibers were loosely held by the matrix material. These results may suggest that debonding between the fibers and matrix or, in other words, fracture occurring in the interface between the fiber and matrix due to poor interfacial adhesion could be the dominant mechanism of failure for this loading mode.

In the case of glass mat fabric laminates, from a closer investigation of the fracture surface [Fig. 8(b)], it is apparent that a number of fibers and bundles protruded from the fracture plane. The pullout fibers had clean surfaces without adhered polymer. It can therefore be concluded that the samples had adhesive failure in the single-fiber pullout region at the interface. On the contrary, a higher magnification showed the bundle to be covered with the matrix, indicating a higher interfacial strength. This fracture surface indicated a brittle failure process with less longitudinal splitting.

CONCLUSIONS

On the basis of observations during tensile testing, the stress–strain curves of polyester composites reinforced with woven roving glass fabric were linear in the direction of the fibers. However, in the matrix-dominated orientations, a nonlinear relation between the stress and strain was observed. The ultimate strength of laminates was lost in the matrix-dominated orientations because of the matrix-controlled failure mode.

For the woven roving glass fabric laminate, the experimental data did not allow an adequate description of the orthogonal model. The difference between the tensile strength values in the two orthogonal directions (in this particular instance, MD and CD) is believed to be due to the fact that the nominal warp and weft directions of the fibers were not controlled during the laminate fabrication by the VARTM process.

We would like to draw attention to the fact that some conclusions of this study refer to the special problem discussed. A possible explanation for the variation of the flexural strength of the glass mat laminate in the test directions performed could arise from the fact that local inhomogeneities, rather than the general microstructure of the chopped strand mat, control the effectiveness of the flexural properties.

Perhaps the most significant result of this investigation is the strong correlation between the changes in the interlaminar shear strength values and fiber orientation angle in the case of woven roving fabric laminates. The direction of the fibers plays a decisive role in the recorded values of the interlaminar shear strengths.

The interlaminar shear strengths recorded at the time of failure were significantly lower than those obtained from three-point-bending tests at all considered test directions.

In this study, a more detailed description, including actual photographs of fractured tensile specimens, of the dependence of the fracture surface on the geometric variables of the fibers is provided. Photographs of fracture surfaces of multiaxial composites loaded in tension along the fiber direction exhibit pronounced irregularity and fiber pullout.

Composites broken in tension and observed under different moderate magnification levels showed uncoated fiber ends pulled from the polymer. The clean fiber surfaces on debonding cracks indicate extensive interfacial failure. The fibers are loosely held by the matrix material after failure.

References

1. Waring, L. A. R. In Glass Reinforced Plastics; Parkyn, B., Ed.; CRC: Cleveland, OH, 1970.
2. Mouritz, A. P.; Baini, C.; Herszberg, I. Compos A 1999, 30, 859.
3. Chou, T. W.; Ishikawa, T. In Textile Structural Composites; Chou, T. W.; Ko, F. K., Eds.; Elsevier: Amsterdam, 1989; Vol. 3.
4. Ishikawa, T.; Chou, T. W. J Compos Mater 1982, 16, 2.
5. Ishikawa, T.; Chou, T. W. J Mater Sci 1982, 71, 3211.
6. Shembekar, P. S.; Naik, N. K. J Compos Mater 1992, 26, 2226.
7. Gu, H. Mater Des 2007, 28, 704.
8. Yang, B.; Kozey, V.; Adanur, S.; Kumar, S. Compos B 2000, 31, 715.
9. Mouritz, A. P.; Banister, M. K.; Falzon, P. J.; Leong, K. H. Compos A 1999, 30, 1445.
10. Gehde, M.; Ehrenstein, G. W. Proc Annu Tech Conf 1991, 49, 2518.

11. Kitano, T.; Haghani, E.; Tanegashima, T.; Saha, P. Polym Compos 2000, 21, 493.
12. Lee, N.-J.; Jang, J. Compos Sci Technol 2000, 60, 209.
13. Zhou, X.; Lin, Q.; Dai, G. Polym Polym Compos 2002, 10, 299.
14. Jang, J.; Han, S. Compos A 1999, 30, 1045.
15. Cantwell, W. J. J Compos Mater 1996, 30, 1266.
16. Wakeman, M. D.; Cain, T. A.; Rudd, C. D.; Brooks, R.; Long, A. C. Compos Sci Technol 1999, 59, 709.
17. Lee, N.-J.; Jang, J. Compos A 1999, 30, 815.
18. Lee, N.-J.; Jang, J. Compos Sci Technol 1997, 57, 1559.
19. Priya, S. P.; Ramakrishna, H. V.; Rai, S. K.; Rajulu, A. V. J Reinforced Plast Compos 2006, 25, 141.
20. Rao, G. B.; Reddy, R. L.; Balaji, P. J.; He, J.; Zhang, J.; Rajulu, A. V. J Reinforced Plast Compos 2002, 21, 577.
21. Seemann, W. H. U.S. Pat. 4,902,215 (1990).
22. Seemann, W. H. U.S. Pat. 5,316,462 (1994).
23. Dexter, H. B. Proc Int SAMPE Tech Conf 1996, 28, 404.
24. Ericson, M.; Berglund, L. Compos Sci Technol 1992, 43, 269.